CrossMark

RESEARCH ARTICLE

Simultaneous prediction of delamination and surface roughness in drilling GFRP composite using ANN

Rasmi Ranjan Behera[1] · **Ranjan Kr. Ghadai**[2] ·
Kanak Kalita[3] · **Simul Banerjee**[4]

Abstract Delamination in the drilling of polyester composite reinforced with chopped fiberglass is a problematic phenomenon. The material's structural integrity is reduced by delamination, which results in poor tolerance during assembly and is a primary reason for decreased performance. Surface roughness is another important factor to consider when drilling fiber-reinforced plastics, as surface roughness causes failures by inducing high stresses in rivets and screws. Due to the random orientation of fiberglass and the non-homogenous, anisotropic properties of this material, an exact mathematical model has not been developed yet. Instead, modelling by artificial neural networks (ANNs) is adopted. In the present work, a multilayer perception ANN architecture has been developed with a feed-forward back-propagation algorithm. The algorithm uses material thickness, drill diameter, spindle speed, and feed rate as input parameters and delamination factor (F_d) at the

✉ Kanak Kalita
  kanakkalita02@gmail.com

  Rasmi Ranjan Behera
  rasmi.behera@gmail.com

  Ranjan Kr. Ghadai
  ranjankumarbls@gmail.com

  Simul Banerjee
  simul_b@hotmail.com

[1] Department of Mechanical Engineering, Indian Institute of Technology, Guwahati 781039, Assam, India

[2] Department of Mechanical Engineering, Sikkim Manipal Institute of Technology, Majitar, Sikkim 737136, India

[3] Department of Mechanical Engineering, MPSTME, SVKM's Narsee Monjee Institute of Management Studies (NMIMS), Shirpur Campus, Dhule, Maharashtra 425405, India

[4] Department of Mechanical Engineering, Jadavpur University, Kolkata, West Bengal 700032, India

entrance of the drilled hole, average surface roughness (R_a), and root mean square surface roughness (R_q) as the output parameters. The ANN model is then used to develop response surfaces to examine the influence of various input parameters on different response parameters. The developed model predicts that surface roughness increases with increases in feed rate and that a smaller-diameter drill will be advantageous in reducing surface roughness. A reduced feed rate will minimize delamination as well.

Introduction

Fiber reinforced plastic (FRP) composites are widespreadly used in structural applications where weight is a prime concern. FRP composites are often preferred over other materials for buildings, rocket exhausts, in aerospace and automobile applications due to their high specific strength. FRP composites are lightweight yet very strong and have high fatigue limit, excellent damping, low thermal expansion and are resistant against corrosion [1]. Composite materials consist of two distinct phases- a continuous the matrix which surrounds the reinforcement or the dispersed phase. Epoxy resins and polyesters resins are extensively used as a matrix in composites due to their unique balance of chemical and mechanical properties as well as wide versatility of treatment. Glass fibres have high specific strength and hence are among the most preferred structural materials.

Owing to their anisotropic and non-homogeneous properties, composite materials show very unique mechanics during cutting [2]. Drilling is a frequently used process during assembly of structures and as much as 100,000 holes are drilled in a small aeroplane to accommodate fasteners. Surface roughness is a significant trait related with drilling of FRP. Surface roughness can give rise to high stresses on fasteners and may lead to failure [3]. Delamination is a commonly encountered problem while drilling FRP composites. Delamination leads to poor assembly tolerance, and is a prime reason in reducing the overall long term performance of composite laminates [4]. As much as 60 % of the totals rejections during the final assembly of the aircraft in an aeroplane industry is due to delamination [5].

According to [3] while using traditional high speed twist drills on GFR epoxy composite the surface roughness can be improved by employing higher cutting speed and high fiber volume fraction. The effect of several drilling and material parameters on delamination, torque and thrust force has been studied by [5]. The influence of geometry and material of tool on thrust force and delamination while drilling a glass fibre reinforced epoxy composites was investigated by Abrao et al. [6]. Velayudham and Krishnamurthy [7] have investigated the influence of point geometry on delamination and thrust force while drilling glass/phenolic-woven fabric composite using cemented carbide drills of different geometries such as normal point geometry tipped carbide drill, web thinned tipped carbide drill and tripod geometry solid carbide drill. Rubio et al. [8] used high-speed machining to

achieve high performance drilling of glass fibre reinforced composites. A complete analysis on delamination of glass fibre reinforced composites for various drills has been reported by Hocheng and Tsao [9].

So far several techniques have been used to study delamination and surface roughness. Palanikumar et al. [10] studied the problem of delamination in drilling glass fibre reinforced epoxy composites with two types of cutting tools: a twist drill and a four flute cutter made of high speed steel using Taguchi's experimental design method as well as response surface regression method. Mohan et al. [11] and Babu et al. [12] used the Taguchi methodology to investigate the delamination in the drilling process of fiber glass reinforced polyester composites. Davim et al. [13] used orthogonal array and analysis of variance to study the cutting characteristics of cemented carbide drills on FRP composite materials. They [14] also studied the behaviour of two separate drill geometries when machining a glass fiber reinforced plastic.

Khashaba et al. [15] examined the effect of speed of drilling and feed rate on the forces and torques required to cut and delamination in drilling chopped GFR composites with different volume fractions of fiber using multi variable linear regression analysis.

Artificial neural network (ANN) is an approach in which a mathematical model is used to mimic the biological neurons. ANN paradigm offers a fast, efficient, reliable and cost-effective process modelling. Neural networks can learn the mathematical mapping between input and output parameters even for nonlinear problems and hence are very flexible and reliable [16, 17]. In addition, it has been reported that the ANN models can provide improvement of 40–70 % on experimental error compared to RSM methods [18]. Bezerra et al. [19] carried out an investigation on carbon fibre/epoxy and glass fibre/epoxy composites for the prediction of shear stress–strain behaviour using a multi-layered neural network which uses Levenberg–Marquardt learning algorithm. Hayajneh et al. [20] used a feed forward back propagation ANN model to study the effect of certain variables on the cutting torque and thrust force in the drilling of self-lubricated alumina/aluminium/graphite hybrid composites.

Kadi [21] has presented an extensive review on mechanical modelling of FRP composites using artificial neural network. Karnik et al. [22] developed an ANN model for the analysis of delamination in high speed drilling of CFRP composite materials. A multi-layer feed forward artificial neural network architecture, trained using EBPTA was used for the prediction of delamination factor at the drill entrance. Tsao and Hocheng [23] used Taguchi method and ANN to predict and evaluate thrust force and roughness of surface in drilling CFRP laminates. Hansda and Banerjee [24] performed a Grey relational analysis on glass fibre reinforced polyester composite to study the effect of several process parameters on Delamination factor and average surface roughness. They [25] have also performed a similar analysis using utility concept with Taguchi's Approach. Soren et al. [26] used the Taguchi Loss Function to analyze the process parameters involved in drilling of GFRP Composites. Rajamurugan et al. [27] developed some empirical relationships between the drilling parameters and delamination for GFR–polyester composites. Mishra et al. [28] estimated the residual tensile strength in uni-directional glass fiber reinforced plastic laminates using an ANN scheme.

Tsao [29] compared response surface method and radial basis function network in drilling CFR laminates. A comprehensive survey of published works on machining of composite laminates with special focus on drilling of GFRP and CFRP was carried out by Abrao et al. [30]. The effect of tool material, geometry and machining parameters on thrust force, torque and delaminating has been studied. It has been reported that out of the total literature on polymeric composites glass fibre reinforced epoxy composites accounts for 50 %. CFR epoxy composites and GFR polyester composites are the next most studied topics. If the published literature is classified as per fibre shape, woven composites features in about 60 % of the works followed by unidirectional fibres and chopped fibres with 20 % each. Another such recent review on delamination in composites provides useful insight on the topic [31]. Apart from this specific application in delamination, ANN has been used by researchers to predict material properties in composites [32–34] and other biomaterials [35–38].

Although there has been a number of notable contributions in the field of drilling in FRP composites, there is still some lacuna which present a good scope for study. One of the areas where there is still much scope of work to be done is the drilling of chopped GFRP laminates as very little work has been done on this material amongst all the FRP laminates. Also application of neural network for simultaneous prediction of delamination and surface roughness during drilling of this material has not been done in any literature. In the present investigation, therefore back propagation neural network is applied for simultaneous prediction of delamination factor at the entry side of hole and surface roughness during drilling of chopped GFRP laminates.

Methodology of artificial neural network (ANN) modelling

In the present study, delamination factor and surface roughness in drilling is predicted by using a multi-layer feed forward Artificial Neural Network. The error back propagation training algorithm (EBPTA) was used to train the ANN. Training patterns i.e. a set of input parameters and output responses are used in the EBPTA, which is a supervised learning based on the generalized delta rule [39, 40]. The connection weights are determined during the ANN training phase. Proper connection weights are extremely important to get high accuracy.

Initially an input–output database is built to train the ANN model based on the data from the drilling experiments. In order to reduce the cost associated and time consumed in experimentation, it is quintessential to plan the experiments such that the trained ANN model would have a comprehensive knowledge of drilling process over the selected range of parameters. Therefore, an experiment scheme based on full factorial design (FFD) was selected using MINITAB software. The developed experimental database was then utilized to train multi-layer neural network using EBPTA.

Experimental details

In the current study, each of the identified factors are assigned three levels as illustrated in Table 1. The experiment scheme based on FFD contains 81 sets of

Table 1 Factors and levels selected for drilling GFRP composites

Factors	Levels		
	1	2	2
Material thickness, t (mm)	8	12	16
Drill diameter, D (mm)	10	12	14
Spindle speed, N (rpm)	400	800	1100
Feed rate, f (mm/rev)	0.1	0.175	0.275

Table 2 Composition of GFRP laminate

Matrix	Polyester
Hardener	Methylethyl ketone peroxide
Reinforcing	E-glass, chopped strand mat (450 g/m^2)

Table 3 Composition of HSS tool material (wt%)

| C	Cr	Mo	W	V
0.9	4.2	5.0	6.4	1.8

drilling process parameter combinations. All the experiments based on full factorial design (FFD) were carried out on a on a The American Tool Works Co., USA make radial drilling machine. The radial drilling machine powered by a 5.5 kW drive motor has a maximum speed of 1500 rpm with variable feed 0.1–0.625 mm/rev. The maximum radial dimension of the work piece is 1475 mm.

The GFRP composite used in the experiment was procured from VMT Glass Fibre Roofing Industries. The composite laminate of the composition as shown in Table 2 was prepared by using the hand layup technique to reinforce chopped strand mat E-glass fibre in polyester resin. The tensile strength of the composite GFRP with glass fiber volume fraction of 0.33 is 700 kg/cm^2. The Barcol hardness of the composite laminate is 40.5. The experiments were performed on 150 mm × 150 mm GFRP samples with wood as the backing material.

Addison & Co. Ltd., India make High Speed Steel taper shank twist drills were used in the drilling operations. This was in accordance with IS: 5103-1969/ISO: 235-1980/DIN: 345-1978/BS: 328: Part 1-1986 specifications. Table 3 lists the chemical composition of the High Speed Steel tool material. The twist drills of 10 mm (flute length: 87 mm: overall length: 168 mm), 12 mm (flute length: 101 mm: overall length: 182 mm) and 14 mm (flute length: 108 mm: overall length: 189 mm) diameters of Grade M2 were used.

In order to avoid any vibrations or displacements occurring during the drilling operation a clamping system was used to fix the composites at the machine centre.

A Carl Zeiss Ltd. make toolmakers' microscope with 30× magnification was also used to measure the damage around the holes at the entrance. The delamination factor is determined, and is given as
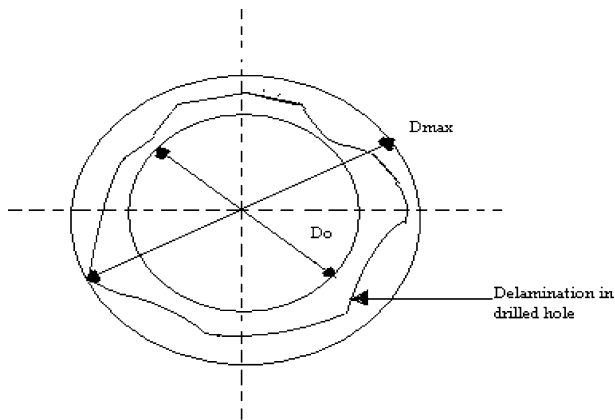
Fig. 1 Scheme for the delamination factor (F_d)

$$F_d = \frac{D_{max}}{D_0} \tag{1}$$

where D_{max} is the maximum diameter of the damaged zone, and D_0 is the diameter of the hole. To reduce any experimental or human errors, three readings for each test were made and the average of delamination factor was considered to be the process response. Figure 1 illustrates the scheme of measuring the delamination factor.

A Taylor Hobson Precision Surtronic 3+ Roughness checker was used to measure the surface roughness parameters over the drilled surfaces. The average surface roughness (R_a) and root mean square surface roughness (R_q) are the considered surface roughness parameters. The surface finish of the work material was measured with 0.8 mm cut-off length. The value of surface roughness parameter R_a and R_q for each experiment were obtained directly from the Taly-profile software integrated with the machine. The average of three readings was taken as the process response. Out of 81 experimental data 72 data were used for the training the network and rest 9 data were used for testing the network. Tables 4 and 5 show the training and testing data for the artificial neural network, respectively.

Artificial neural network

The neurons in the multi-layer feed forward artificial neural network are divided as input layer, output layer and hidden layers. The information regarding the input–output relationship are stored in the links connecting the layers, which stores the knowledge regarding the input–output relationship.

Figure 2 depicts the architecture of the multi-layer feed forward ANN, which consists of four neurons in the input layer (corresponding to 4 process inputs, t, D, N and f), three neurons in the output layer (corresponding to three outputs, F_d, R_a and R_q) and two hidden layers. The net activation input for ith neuron in the hidden and output layer is calculated by

Table 4 Training data for ANN

Experiment number	Material thickness (mm)	Drill diameter (mm)	Spindle Speed (rpm)	Feed rate (mm/rev)	Delamination factor (F_d)	R_a (μm)	R_q (μm)
1	16	10	400	0.275	1.2547	4.747	5.857
2	16	10	400	0.100	1.1402	4.103	5.263
3	8	12	1100	0.175	1.2536	4.083	5.343
4	8	10	1100	0.100	1.2073	3.473	4.562
5	16	14	1100	0.275	1.2539	5.450	6.687
6	12	12	800	0.175	1.2099	4.171	5.297
7	8	14	800	0.175	1.2762	4.253	5.493
8	12	14	800	0.100	1.1956	3.673	4.762
9	8	10	400	0.100	1.2239	3.497	4.602
10	16	12	400	0.100	1.1001	4.043	5.203
11	8	12	1100	0.100	1.2051	3.883	5.217
12	12	10	400	0.100	1.1862	3.332	4.277
13	16	12	800	0.175	1.1841	4.513	5.507
14	16	12	800	0.100	1.1324	3.553	4.631
15	12	10	1100	0.175	1.2202	3.753	4.703
16	12	14	800	0.275	1.2908	4.204	5.583
17	12	10	1100	0.100	1.1735	3.160	4.247
18	8	14	800	0.275	1.3373	4.937	6.230
19	12	12	1100	0.100	1.1643	3.980	4.927
20	16	10	1100	0.175	1.1743	4.171	5.307
21	8	10	1100	0.275	1.3183	4.623	5.902
22	8	14	400	0.100	1.2210	3.130	4.207
23	16	14	1100	0.100	1.1358	4.273	5.523
24	16	10	1100	0.100	1.1387	3.513	4.403
25	16	12	1100	0.100	1.1409	4.273	5.467
26	16	14	1100	0.175	1.1864	4.957	6.513
27	16	14	800	0.100	1.1404	4.340	5.841
28	8	14	1100	0.100	1.2339	4.037	5.157
29	8	10	400	0.275	1.3283	3.733	4.803
30	8	14	400	0.275	1.3336	5.277	6.873
31	8	12	1100	0.275	1.3183	4.450	5.593
32	16	10	400	0.175	1.1893	4.423	5.692
33	16	12	1100	0.275	1.1994	5.173	6.701
34	8	10	800	0.275	1.3259	4.223	5.442
35	16	14	400	0.100	1.1251	3.803	4.893
36	12	14	400	0.275	1.2924	4.777	5.817
37	16	12	400	0.275	1.2218	5.073	6.28
38	16	10	800	0.100	1.1225	3.871	4.997
39	12	12	800	0.100	1.1557	3.845	5.105
40	8	10	800	0.175	1.2622	3.947	4.943

Table 4 continued

Experiment number	Material thickness (mm)	Drill diameter (mm)	Spindle Speed (rpm)	Feed rate (mm/rev)	Delamination factor (F_d)	R_a (μm)	R_q (μm)
41	8	12	400	0.175	1.2868	3.653	4.507
42	12	12	400	0.275	1.2503	4.353	5.457
43	16	14	400	0.275	1.2116	5.317	6.937
44	16	14	400	0.175	1.1622	4.697	6.037
45	12	14	800	0.175	1.2364	3.957	4.983
46	16	12	1100	0.175	1.1660	4.457	5.860
47	12	10	800	0.100	1.1617	3.437	4.403
48	8	14	1100	0.275	1.3257	4.633	5.743
49	12	12	1100	0.175	1.2197	4.317	5.083
50	8	14	400	0.175	1.2692	4.421	5.742
51	12	12	1100	0.275	1.2934	4.563	5.703
52	16	10	800	0.175	1.1768	4.227	5.467
53	8	12	800	0.275	1.3643	4.297	5.553
54	16	10	800	0.275	1.2493	4.527	5.627
55	8	10	400	0.175	1.2687	3.583	4.682
56	8	10	1100	0.175	1.2549	4.127	5.347
57	12	10	800	0.175	1.2058	3.953	5.007
58	8	12	400	0.100	1.2287	3.412	4.197
59	16	14	800	0.275	1.2486	5.813	7.243
60	16	12	800	0.275	1.2530	4.817	5.983
61	12	14	400	0.175	1.2157	4.513	5.683
62	12	10	400	0.275	1.2849	4.213	5.272
63	12	14	1100	0.275	1.2898	5.504	6.833
64	12	14	400	0.100	1.1582	3.883	4.873
65	8	10	800	0.100	1.2145	3.707	4.420
66	12	14	1100	0.175	1.2406	5.023	6.393
67	12	14	1100	0.100	1.2037	4.283	5.233
68	12	12	800	0.275	1.2819	4.393	5.457
69	12	10	400	0.175	1.2264	3.907	4.787
70	12	12	400	0.100	1.1527	3.567	4.290
71	8	12	400	0.275	1.3583	4.672	5.697
72	8	14	800	0.100	1.2304	3.863	4.950

$$net_i = \sum_j w_{ij} o_j \tag{2}$$

where w_{ij} is the weight of link connecting neuron j to i and O_j is the output of *j*th neuron in the previous layer.

The output of *i*th neuron for a unipolar sigmoid activation function, is given as

Table 5 Testing data for ANN

Experiment number	Material thickness (mm)	Drill diameter (mm)	Spindle speed (rpm)	Feed rate (mm/rev)	Delamination Factor (F_d)	R_a (µm)	R_q (µm)
1	12	10	800	0.275	1.2647	4.280	5.450
2	12	12	400	0.175	1.1945	4.083	5.193
3	12	10	1100	0.275	1.2623	4.127	5.177
4	8	12	800	0.100	1.2789	3.703	4.657
5	16	10	1100	0.275	1.1917	4.507	5.587
6	8	12	800	0.175	1.2844	3.961	5.053
7	16	14	800	0.175	1.1867	5.173	6.663
8	8	14	1100	0.175	1.2332	4.327	5.307
9	16	12	400	0.175	1.1523	4.561	5.713
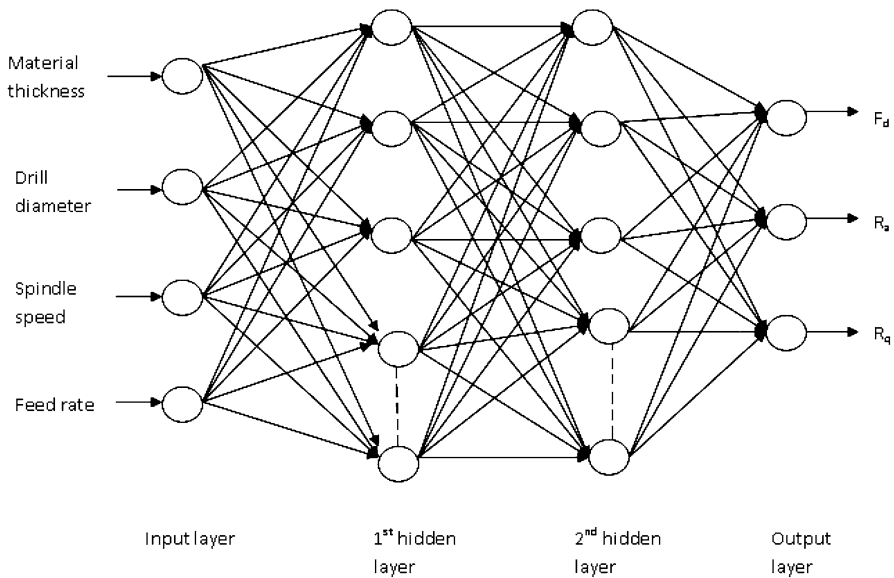
Fig. 2 Architecture of the neural network model for double hidden layer

$$o_i = \frac{1}{1 + e^{-\lambda net_i}} \quad (3)$$

where λ is the scaling factor.

To minimize the sum of squared error for k-number of output neurons the EBPTA uses weight updates and is given by

$$E = \frac{1}{2} \sum_{k=1}^{k} (d_{k,p} - o_{k,p})^2 \quad (4)$$

where $d_{k,p}$ = desired output for the pth pattern. The weights of the links are updated as

$$w_{ji(n+1)} = w_{ji(n)} + \eta \delta_{pj} o_{pi} + \alpha \Delta w_{ji(n)} \tag{5}$$

where n is the learning step, η is the learning rate and α is the momentum constant.

In Eq. (5), δ_{pj} is the error term, which is given as follows:

$$\text{For output layer}: \quad \delta_{pk} = (d_{kp} - o_{kp})(1 - o_{kp}); \ k = 1, \ldots, K \tag{6}$$

$$\text{For hidden layer}: \quad \delta_{pj} = o_{pj}(1 - o_{pj}) \sum \delta_{pk} w_{kj}; \ j = 1, \ldots, J \tag{7}$$

where J is the number of the neurons in the hidden layer.

Small random weight values are assigned to all the links during the initialization of the training process. The input–output patterns are presented at a time. The mean square error due to all patterns is computed as

$$MSE = \frac{1}{NP} \sum_{p=1}^{NP} \sum_{k=1}^{K} (d_{kp} - o_{kp})^2 \tag{8}$$

where NP = number of training patterns.

The training process is terminated when the predefined MSE or maximum number of epochs is realised.

Artificial neural network training

The neural network toolbox available in MATLAB was used to train the ANN for 72 input–output patterns. The simulated multi-layer feed forward ANN architecture
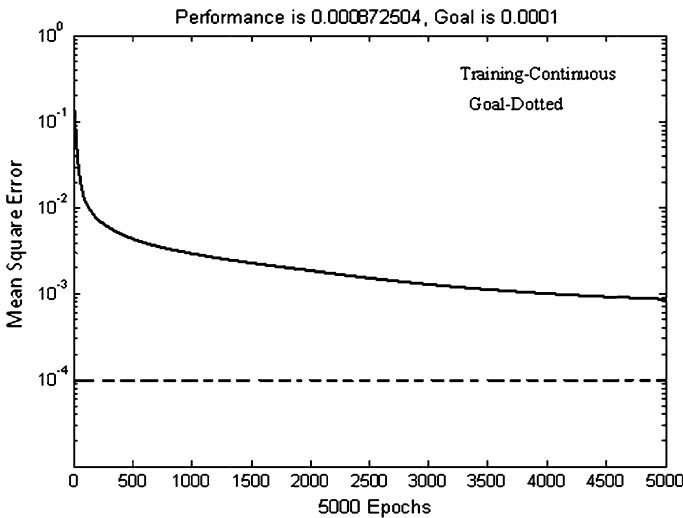
Fig. 3 A typical training progress of the ANN model
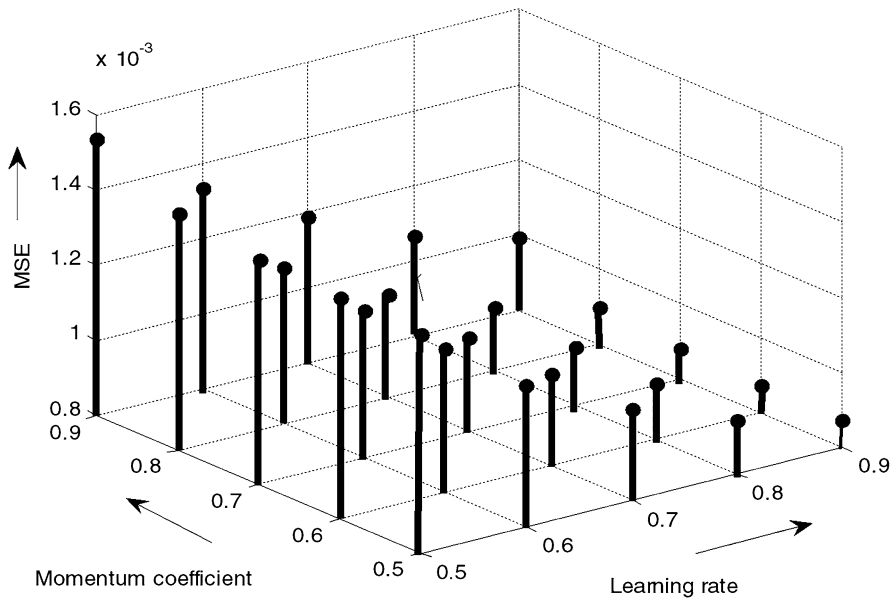
Fig. 4 Number of hidden neurons in 1st and 2nd layer = 13 & 13

consists of 4 neurons in the input layer and 3 neurons in the output layer. Normalization of all the inputs and desired outputs are carried out using the expression

$$X_{norm} = 0.1 + 0.8 \left(\frac{X - X_{\min}}{X_{\max} - X_{\min}} \right) \tag{9}$$

where X_{norm} = normalized data.

This normalized maps all inputs and desired outputs in the range [0.1:0.9]. The ANN training simulation was carried out using batch gradient descent with momentum training procedure "traingdm" of MATLAB NN toolbox.

The number of neurons used in the hidden layer during training of artificial neural network is extremly important as it has been seen that using fewer neurons leads to substandard approximation and exceesive neurons in the hidden layer cause over-approximation. Trial and error method is used to determine the 'appropriate number' of neurons in the hidden layer so that the problem of under fitting or overfitting can be avoided. However the 'appropriate number' of neurons needed for accurate prediction of output response is problem specific. It has also been reported that if the artificial neural network is trained beyond a certain number of epochs, the neural network has a tendancy to store the input–output models, which lead to poor generalization ability. So in this study 0.0001 MSE and 5000 epochs were defined as objective of the ANN training [22].

In the present investigation, both single and double hidden layer were considered for the ANN model. Batch mode of training was used for the training the network. Tan-sigmoid activation function and log-sigmoid activation function was used for hidden layer and output layer, respectively. The learning rate and momentum
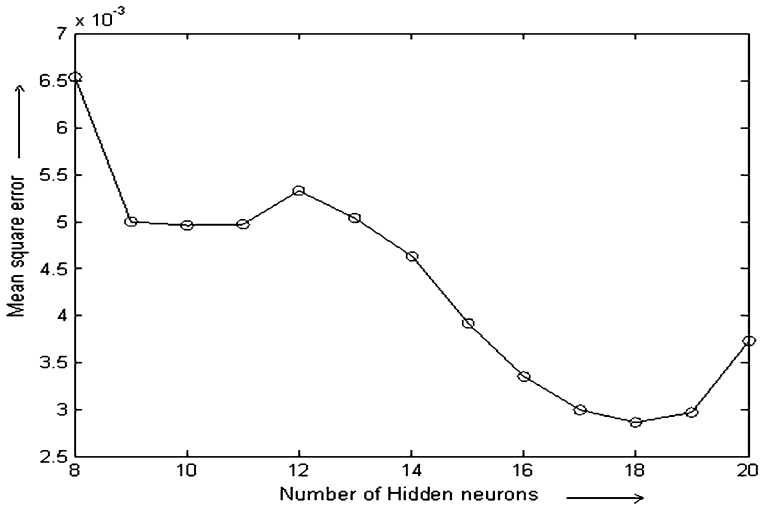
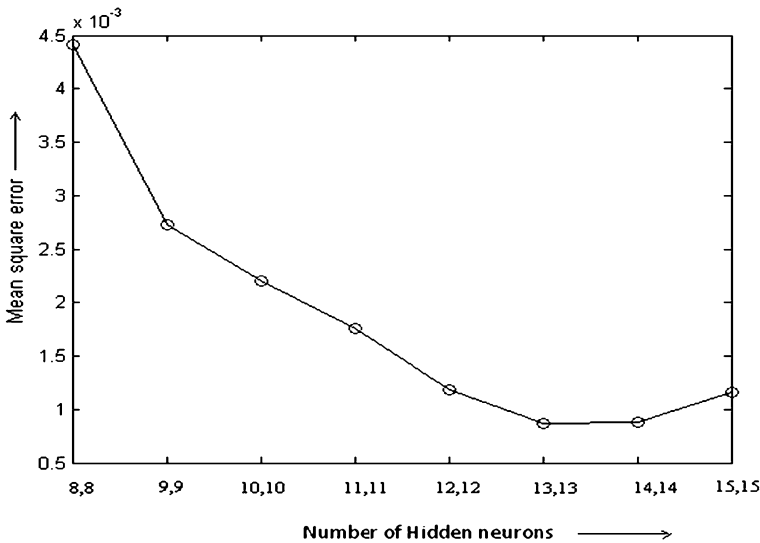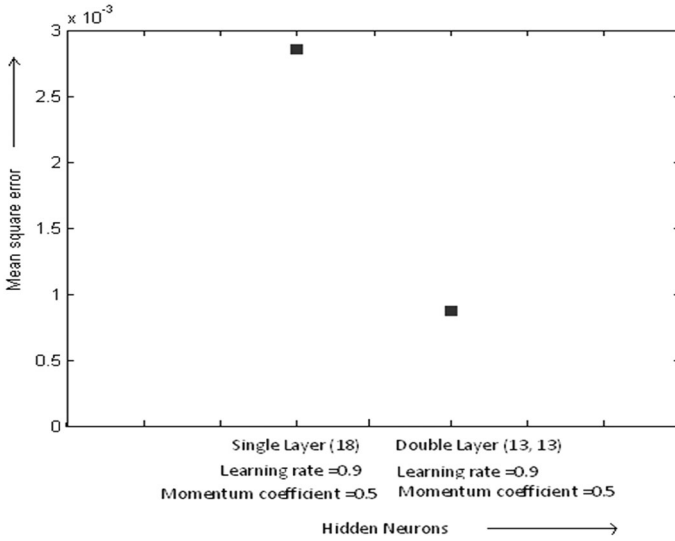**Fig. 5** Comparison of single layer architecture's means square error

Fig. 6 Comparison of double layer architecture's means square error

coefficient were changed between 0.5 and 0.9. Large numbers of neural network architecture were tried with different combination of number of neurons in the hidden layers, learning rate and momentum coefficient. For each architecture 25 combinations of learning rate and momentum coefficient was evaluated. A typical training progress is shown in Fig. 3. The MSE for different combination of learning rate and momentum coefficient of 4-13-13-3 are shown in Fig. 4. The comparison

Fig. 7 Comparison of the minimum value of the single and double layer architecture's mean square error

Table 6 Comparison of optimum architectures for different hidden layers

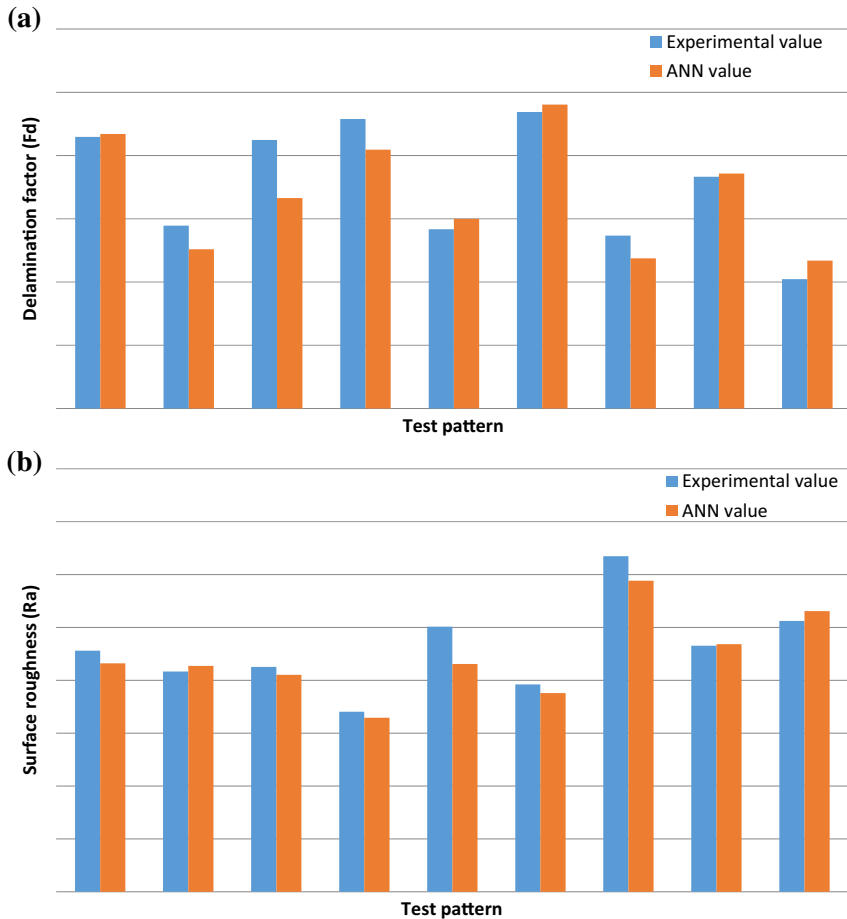| Serial no.	Network architecture	Learning rate	Momentum coefficient	Mean square error after 5000 iterations
1	4-8-3	0.9	0.5	0.006533
2	4-9-3	0.9	0.5	0.004988
3	4-10-3	0.9	0.5	0.004958
4	4-11-3	0.9	0.5	0.004969
5	4-12-3	0.9	0.9	0.005317
6	4-13-3	0.9	0.8	0.005029
7	4-14-3	0.9	0.7	0.004626
8	4-15-3	0.9	0.5	0.003916
9	4-16-3	0.9	0.5	0.003351
10	4-17-3	0.9	0.5	0.002991
11	4-18-3	0.9	0.5	0.002856
12	4-19-3	0.9	0.5	0.002966
13	4-20-3	0.9	0.5	0.003725
14	4-8-8-3	0.9	0.5	0.004418
15	4-9-9-3	0.9	0.8	0.002730
16	4-10-10-3	0.9	0.9	0.002206
17	4-11-11-3	0.9	0.9	0.001759
18	4-12-12-3	0.9	0.5	0.001187
19	**4-13-13-3**	**0.9**	**0.5**	**0.000872**

Table 6 continued

Serial no.	Network architecture	Learning rate	Momentum coefficient	Mean square error after 5000 iterations
20	4-14-14-3	0.9	0.9	0.000879
21	4-15-15-3	0.9	0.9	0.001160

Bold values has the least mean square error, it is used for making all the current predictions reported in the paper

Fig. 8 **a** Correlation of training patterns for F_d. **b** Correlation of training patterns for R_a

(a) Best Linear Fit: A = (0.974) T + (0.0317)

R = 0.987

(b) Best Linear Fit: A = (0.965) T + (0.148)

R = 0.988
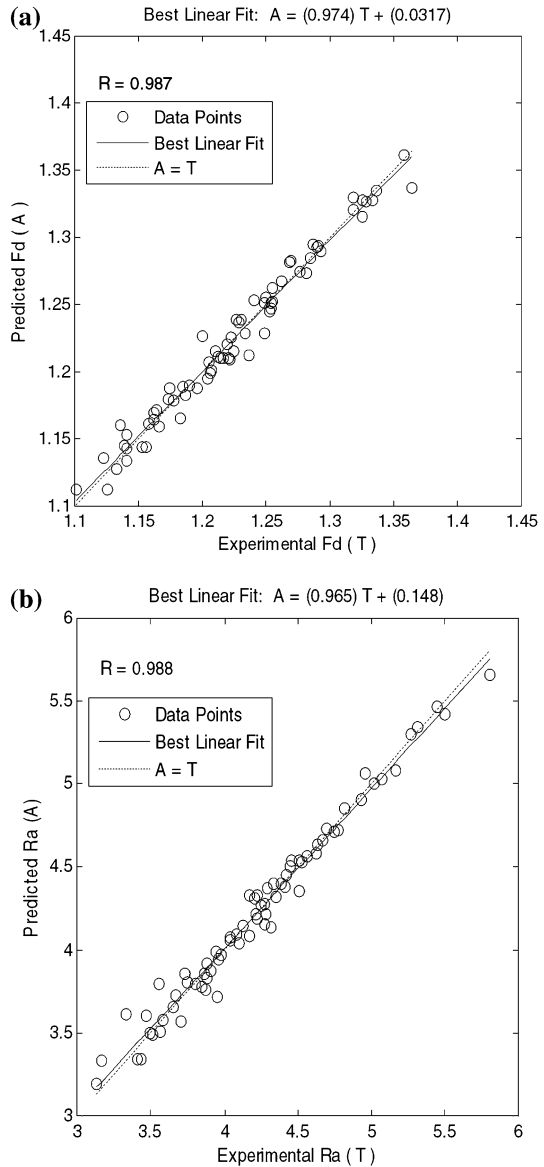
Fig. 9 **a** Comparison between actual and predicted F_d (original value). **b** Comparison between actual and predicted R_a (original value)

between different single and double layer architecture's minimum mean square errors are shown in Figs. 5 and 6 respectively. Figure 7 shows the comparison of the minimum value of the single layer and double layer architecture's mean square error. Table 6 shows the comparison of different architectures. It was found that 4-13-13-3 architecture has the least mean square error of 0.000872504 with learning rate of 0.9 and momentum coefficient of 0.5.

Artificial neural network testing

72 input patterns used during the training were used as the inputs for testing the trained artificial neural network. The predicted values (of the F_d, R_a and R_q) by the trained ANN was compared with the experimental results and absolute prediction error was calculated as,

Table 7 Comparison between experimental and ANN predicted result for testing dataset

Serial no.	F_d actual	F_d predicted by ANN	% Error	R_a actual	R_a predicted by ANN	% Error	R_q actual	R_q predicted by ANN	% Error
1	1.2647	1.2670	0.1836	4.280	4.1609	2.7839	5.450	5.2144	4.3223
2	1.1945	1.1759	1.5589	4.083	4.1355	1.2852	5.193	5.2619	1.3272
3	1.2623	1.2164	3.6323	4.127	4.0524	1.8083	5.177	5.2415	1.2450
4	1.2789	1.2547	1.8920	3.703	3.6469	1.5145	4.657	4.6187	0.8215
5	1.1917	1.2000	0.6932	4.507	4.1547	7.8171	5.587	5.4064	3.2319
6	1.2844	1.2903	0.4592	3.961	3.8797	2.0521	5.053	4.8465	4.0858
7	1.1867	1.1687	1.5154	5.173	4.9417	4.4704	6.663	6.2753	5.8183
8	1.2332	1.2358	0.2078	4.327	4.3421	0.3500	5.307	5.5140	3.9007
9	1.1523	1.1669	1.2666	4.561	4.6543	2.0455	5.713	5.8757	2.8484
	Average prediction error of F_d = 1.27 %			Average prediction error of R_a = 2.68 %			Average prediction error of R_q = 3.07 %		
Overall average prediction error = 2.34 %									

$$\% \text{ Absolute prediction error} = \left| \frac{\text{Actual value} - \text{predicted value}}{\text{Actual value}} \right| \times 100 \qquad (10)$$

The mean absolute prediction error was found to be around 0.63, 1.56 and 1.93 % for F_d, R_a and R_q, respectively for training patterns.

A scatter plot is presented in Fig. 8 which shows a linear the correlation between the experimental and the ANN predicated values. The correlation coefficient (R) between the experimental and the predicted value is an indication of how well the variations in the predicted response values are explained by the targets. It is found that the R values are 0.987, 0.988 and 0.985 for F_d, R_a and R_q, respectively indicating excellent goodness of fit for the training data.

For the validation purpose, testing data were used which do not belong to the training data set. With these input data, the output values were predicted using the ANN model thus developed. The comparison of the predicted and the experimental values of different responses for the testing data are exhibited in Fig. 9 and it can be observed that the predicted response values follow almost the same trend as that of the actual response values. The mean absolute prediction error was found to be around 1.27, 2.68 and 3.07 % for F_d, R_a and R_q, respectively, for the testing data as shown in Table 7. Figure 10 exhibits a linear correlation plot between the experimental and the ANN predicted output values for the testing patterns. It is found that the R values are 0.912, 0.944 and 0.933 for F_d, R_a and R_q, respectively indicating excellent goodness of fit for the testing data.

Results and discussion

The current Artificial Neural Network model can be used for analysing the influence of the selected drilling parameters on response. To understand the combined influence of various drilling parameters on delamination factor (F_d), average surface

**Fig. 10 a** Correlation of testing patterns for F_d. **b** Correlation of testing patterns for R_a
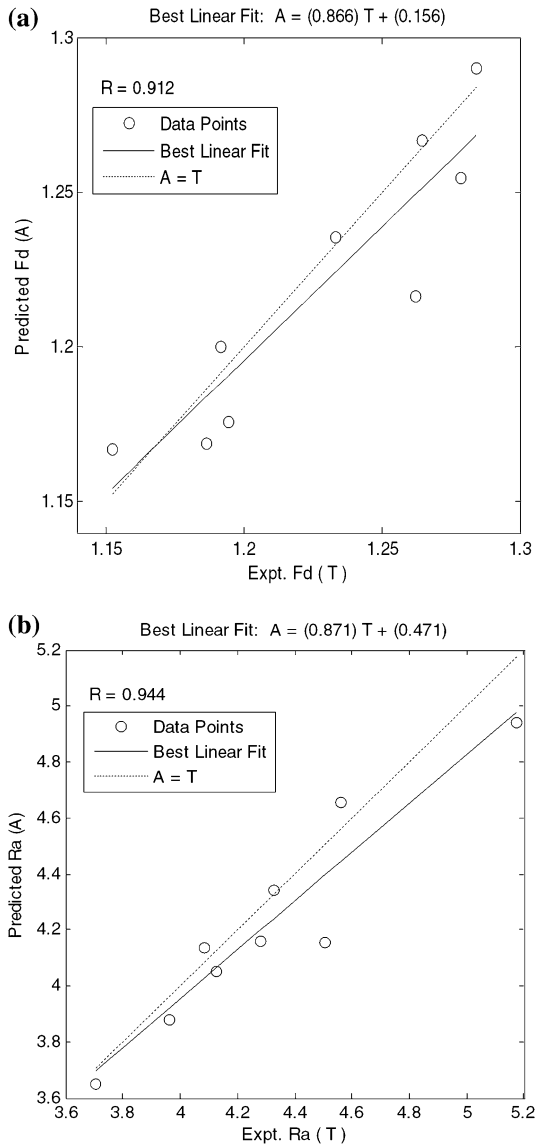
roughness (R_a) and root mean square surface roughness (R_q), three-dimensional surface plots were generated by taking any two parameters at a time, while keeping the third and fourth parameters at level 2. The effect of such interactions are presented in Figs. 11, 12, 13, 14, 15, 16.

Figure 11a shows that the when feed rate is increased, the delamination factor (F_d) sharply irrespective of spindle speed. This is in direct agreement with the experimental findings reported by Rubio et al. [8]. This is due to the fact that higher thrust forces are developed at higher feed rates which in turn causes more

(a)

(b)
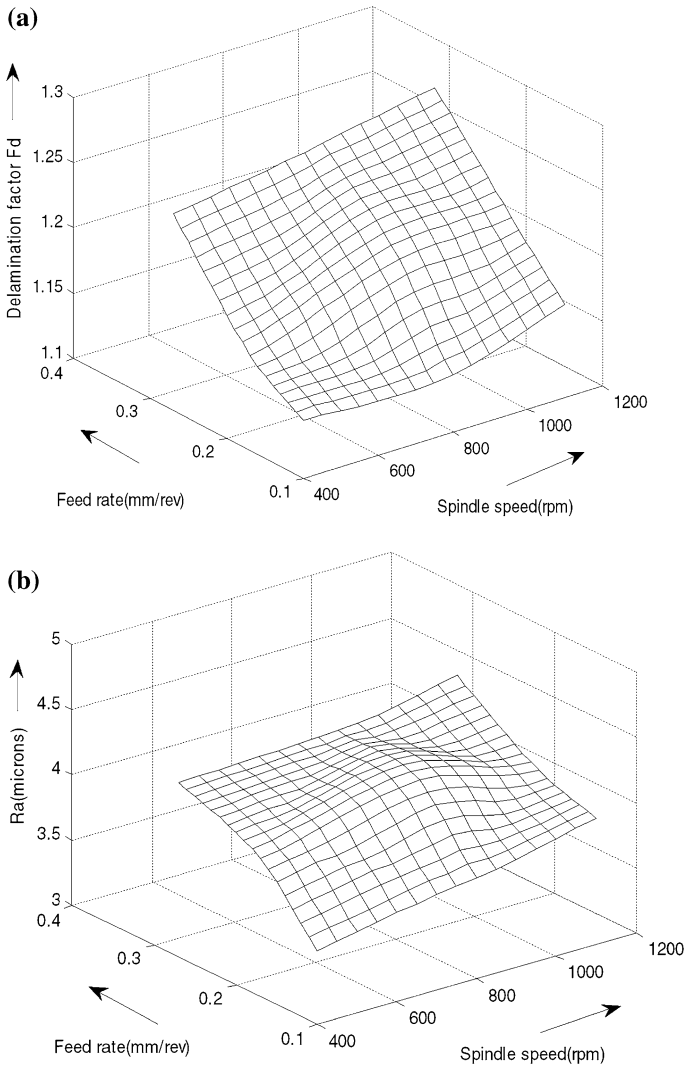
Fig. 11 Effect of f and N on the response parameters at D = 12 mm and t = 12 mm. **a** For delamination factor (F_d). **b** For surface roughness (R_a)

delamination. Though not as sharp as the increase in delamination with respect to feed rate the spindle speed too has an enhancing effect on delamination. At a combined high feed rate and high spindle speed, large amount of delamination is seen. Thus it is seen that feed rate and spindle speed are the most influencing parameters while drilling composites. Vankanti and Ganta [41] had also arrived at the same conclusion using ANOVA. Hansda and Banerjee [24] had also reported that delamination is augmented by increased feed rate. It is observed from Fig. 11b that with increase in feed rates the surface roughness increases monotonically. Also at low feed rates spindle speed has significant influence. It is seen that at low feed
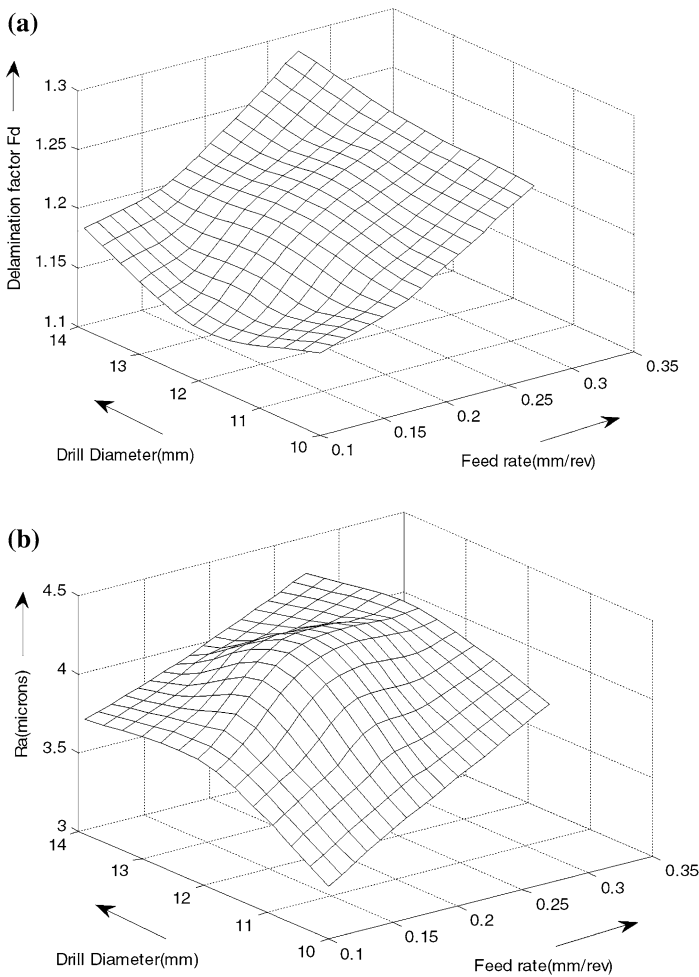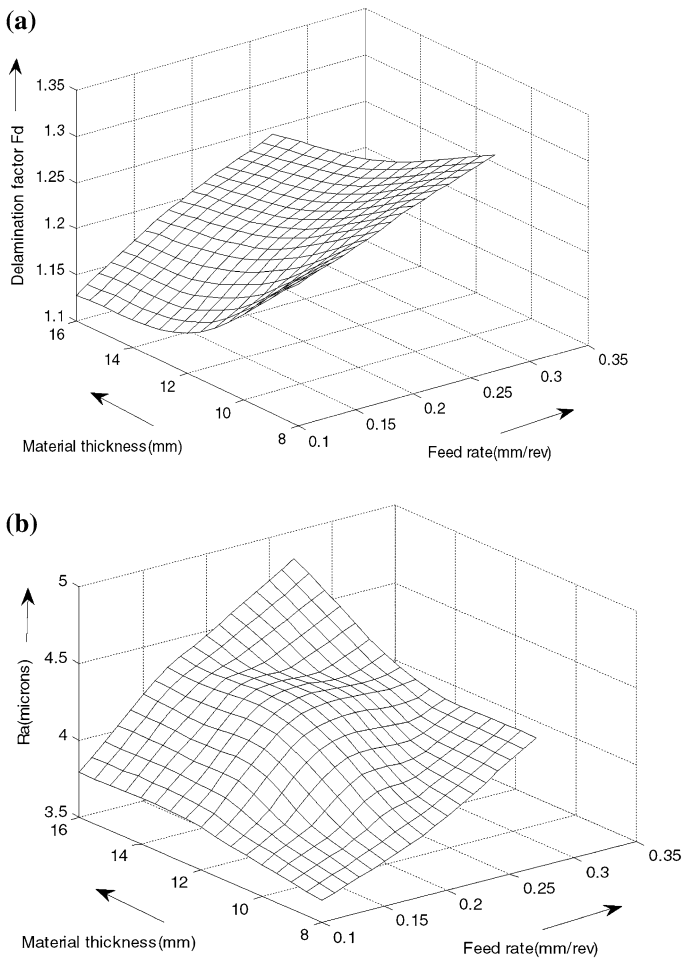
Fig. 12 Effect of D & f on the response parameters at N = 800 rpm and t = 12 mm. **a** For delamination factor (F_d). **b** For surface roughness (R_a)

rates the increase in surface roughness with increase in spindle speed is almost linear. However at higher feed rates the effect is as prominent.

Figure 12a shows that the minimum delamination occurs at the lower level of feed rate irrespective of drill diameter. For any drill size feed rate is a significant parameter as delamination in the FRP increases with feed rate. In Fig. 12b it is observed that when the drill diameter is at centre level, the surface roughness is very sensitive to feed rate. The surface roughness increases monotonically as feed rate is increased. However this rate of increment in surface roughness with respect to feed rate is much higher at low level of drill diameter.

Figure 13a demonstrates that at the higher level of material thickness, the delamination factor is small and sharply decreases from lower level to centre level
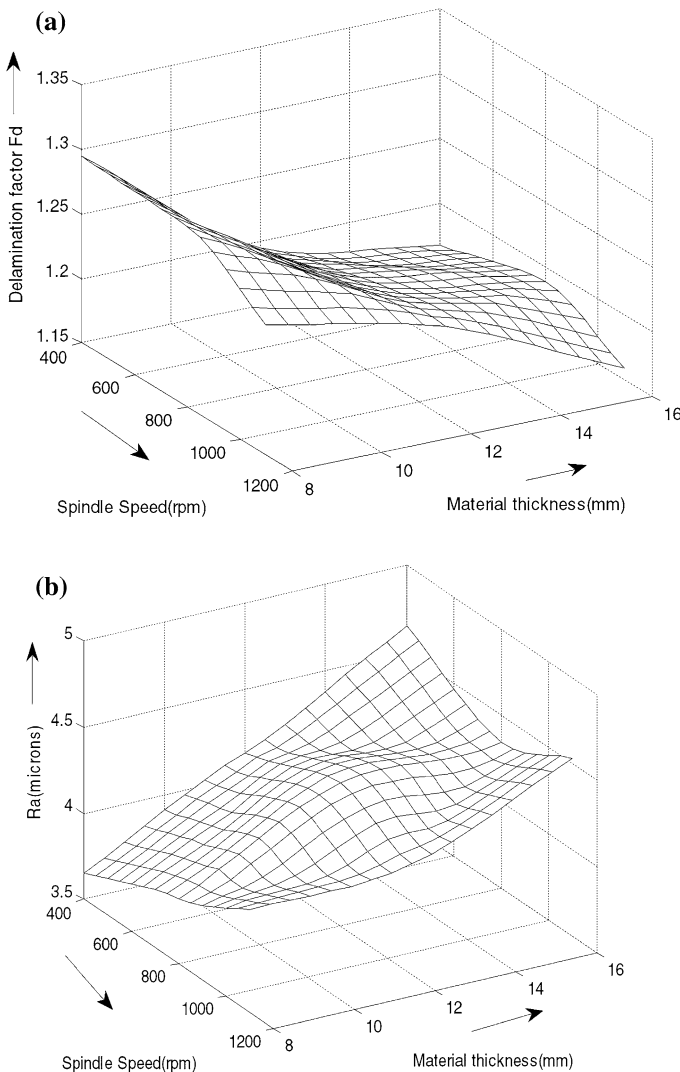
Fig. 13 Effect of t & f on the response parameters at N = 800 rpm and D = 12 mm. **a** For delamination factor (F_d). **b** For surface roughness (R_a)

of material thickness. Delamination is most prominent when material thickness is very low. Also it is observed that higher feed rates are responsible for more delamination. When the material thickness is high, the surface roughness is extremely sensitive to feed rate, as shown in Fig. 13b; it is also seen that, surface roughness varies very little with the change in material thickness at lower feed rate.

The delamination decreases with the increase in material thickness irrespective of spindle speed as shown in Fig. 14a; whereas, the surface roughness increases with increasing material thickness as seen from Fig. 14b.

The delamination factor drops with rise in material thickness with the variations in drill diameter as seen in Fig. 15a. From Fig. 15b, it is obvious that a lesser drill diameter is essential with the changes in material thickness in order to reduce the surface roughness.

Fig. 14 Effect of N & t on the response parameters at f = 0.175 mm/rev and D = 12 mm. **a** For delamination factor (F_d). **b** For surface roughness (R_a)

The least delamination occurs at lower level of spindle speed and centre level of drill diameter as shown in Fig. 16a. From Fig. 16b, it is clear that small drills are advantageous to minimize surface roughness at different spindle speeds.

It is evident that the developed artificial neural network model is extremely useful in investigating the influence of various drilling-process parameters on the response parameters. Using the current ANN model it is very convenient to predict the response parameters for any given set of inputs. The developed ANN model is very versatile and accurate; its accuracy may be increased further by using more

(a)

(b)
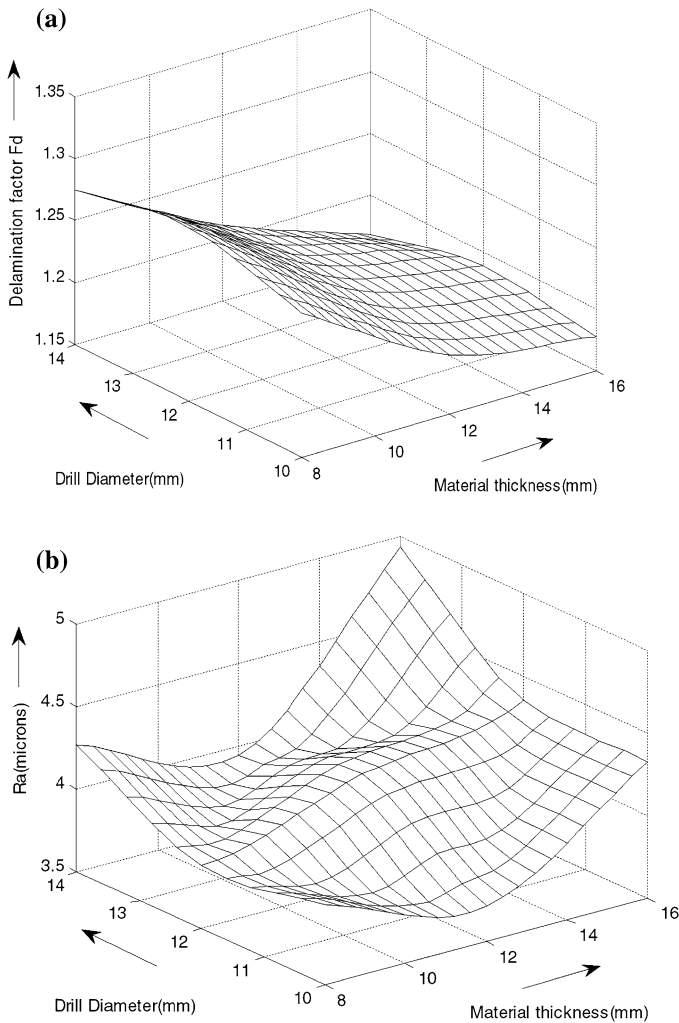
Fig. 15 Effect of D & t on the response parameters at f = 0.175 mm/rev and N = 800 rpm. **a** For delamination factor (F_d). **b** For surface roughness (R_a)

training data patterns. The current ANN model is capable of capturing any non-linearity in input and the output parameters with high generalization ability. Hence by using this model, the combined influence of several drilling parameters can be predicted with high degree of accuracy.

Figure 17a, b shows the SEM micrograph of drilled surface at entry and exit side of the hole respectively under minimum delamination condition. Figure 18a, b shows the same for maximum delamination condition. From Fig. 17 it is seen that the crack propagation is parallel to the surface whereas Fig. 18 reveals that the crack propagation is inclined to the surface. Hence in minimum delamination condition the crack cannot be manifested from the top of the drilled hole but in the maximum

(a)

(b)
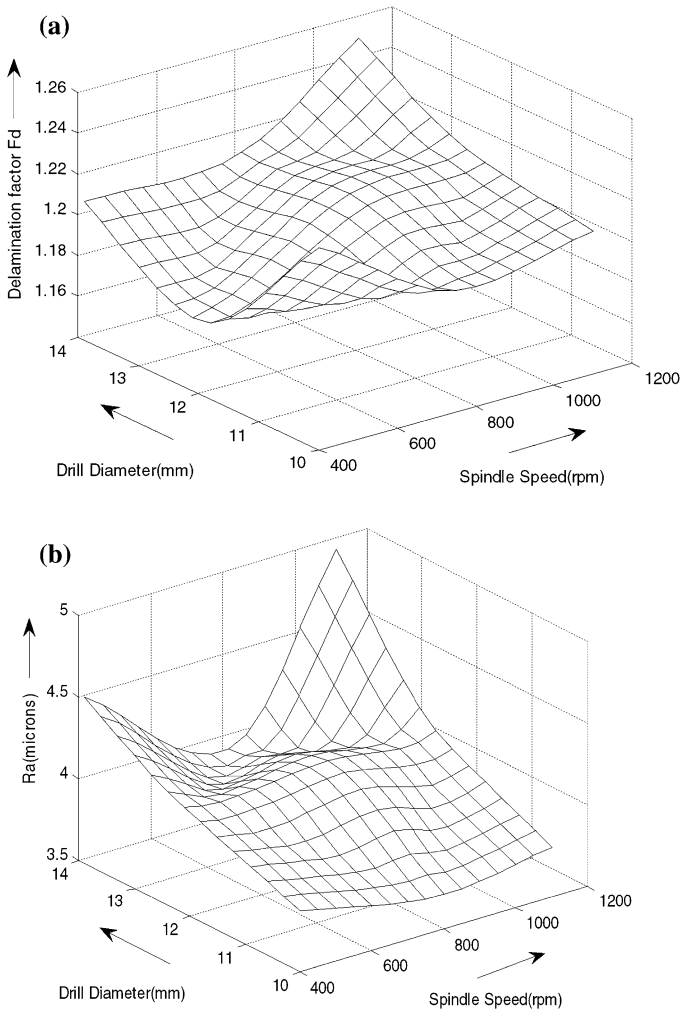
Fig. 16 Effect of D & N on the response parameters at f = 0.175 mm/rev and t = 12 mm. **a** For delamination factor (F_d). **b** For surface roughness (R_a)

delamination condition it is possible. Thus the delamination factor is small for minimum delamination condition but large for maximum delamination condition.

Conclusions

The prime interest of this work was to build an artificial neural network model with very high accuracy to analyse the effect of several drilling constraints on the delamination factor (F_d) and surface roughness during drilling of chopped GFRP composites. Thus the multilayer feed forward ANN model was developed and
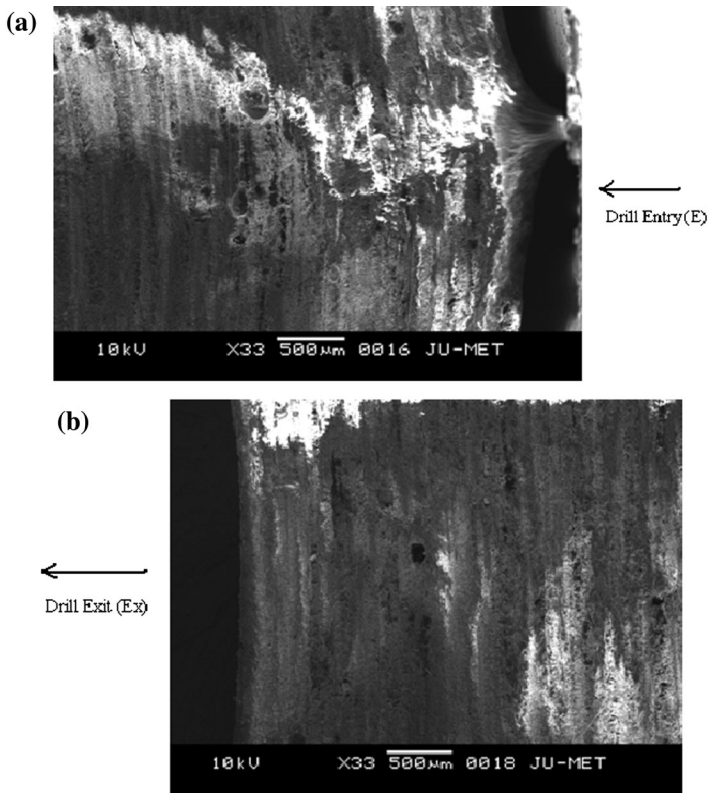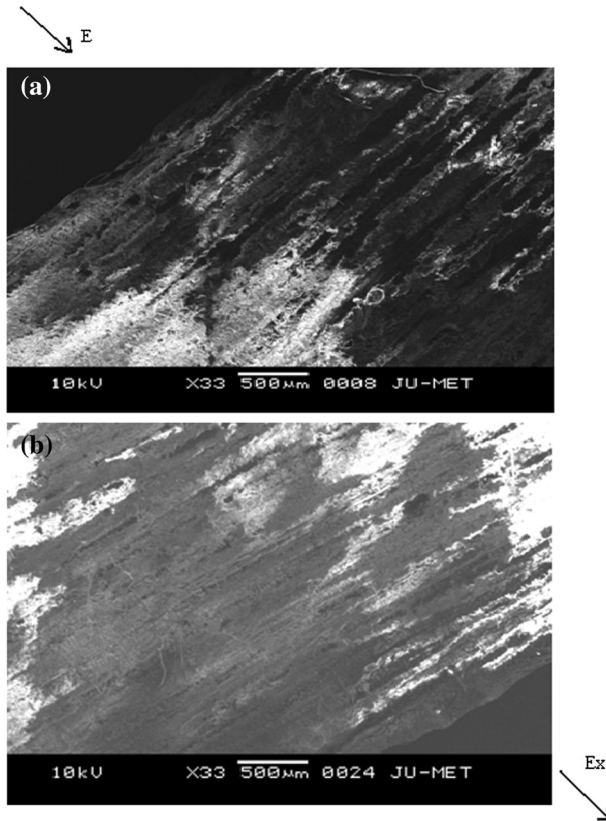
Fig. 17 SEM micrograph of drilled surface of minimum delamination (t = 16 mm, D = 12 mm, N = 400 rpm and f = 0.100 mm/rev). **a** At entry side of drilled surface. **b** At exit side of drilled surface

evaluated. From the experiments and numerical simulations, the following inferences can be drawn,

- The current artificial neural network model shows an extremely healthy correlation between the training and testing datasets, thus confirming the validity of the ANN. The overall difference between experimental results and artificial neural network predictions for training and testing datasets is found to be 1.37 and 2.34 % respectively.
- The response parameters and the selected drilling process parameters have a very high non-linear relationship. The combined effect of the process parameters on both the surface roughness, namely R_a and R_q are quite similar while different from the delamination factor (F_d).
- All the response parameters are very sensitive to all the process constraints with feed rate being the most important parameter.
- Delamination reduces with increase in material thickness and decrease in in feed rate.

Fig. 18 SEM micrograph of drilled surface of maximum delamination (t = 8 mm, D = 12 mm, N = 800 rpm and f = 0.275 mm/rev). **a** At entry side of drilled surface. **b** At exit side of drilled surface

- Both the surface roughness parameters increase with increase in feed rate. Smaller value of drill diameter is required for the minimum surface roughness.
- Feed rate has most significant effect on the response parameters while the spindle speed has negligible effect. The output response are also highly dependent on the material thickness and drill diameter.

References

1. Guu YH, Hocheng H, Tai NH, Liu SY (2001) Effect of electrical discharge machining on the characteristics of carbon fibre reinforced carbon composites. J Mater Sci 36:2037–2043
2. Callister WD (2002) Materials science and engineering: an introduction, 6th edn. Wiley, Mississauga
3. Sonbaty EI, Khasaba UA, Machaly T (2004) Factors affecting the machinability of GFR/epoxy composites. Compos Struct 63:329–338
4. Capello E (2004) Workpiece damping and its effects on delamination damage in drilling thin composite laminates. J Mater Process Technol 148:186–195

5. Khashaba UA (2004) Delamination in drilling GFR-thermoset composites. Compos Struct 63:313–327

6. Abrao AM, Rubio JC, Faria PE, Davim JP (2008) The effect of cutting tool geometry on thrust force and delamination when drilling glass fibre reinforced plastic. Mater Des 29:508–513

7. Velayudham A, Krishnamurty R (2007) Effect of point geometry and their influence on thrust force and delamination in drilling of polymeric composites. J Mater Process Technol 185:204–209

8. Rubio JC, Abrao AM, Faria PE, Correia AE, Davim JP (2008) Effects of high speed in drilling of glass fiber reinforced plastic: evaluation of the delamination factor. Int J Mach Tools Manuf 48:715–720

9. Hocheng H, Tsao C (2003) Comprehensive analysis of delamination in drilling of composite materials with various drill bits. J Mater Process Technol 140:335–339

10. Palanikumar K, Prakash S, Shanmugam K (2008) Evaluation of delamination in drilling GFRP composites. Mater Manuf Process 23:858–864

11. Mohan NS, Kulkarni SM, Ramachandra A (2007) Delamination analysis in drilling process of glass fibre reinforced plastic (GFRP) composite materials. J Mater Process Technol 186:265–271

12. Babu J, Philip J (2014) Experimental studies on effect of process parameters on delamination in drilling GFRP composites using Taguchi method. Proc Mater Sci 6:1131–1142

13. Davim JP, Reis P, Antonio CC (2004) Drilling fibre reinforced plastics (FRPs) manufactured by hand lay-up: influence of matrix (Viapalvup 9731 and ATLAC 382-05). J Mater Process Technol 155:1828–1833

14. Davim JP, Reis P, Antonio CC (2004) Experimental study on drilling glass fibre reinforced plastics (GFRP) manufactured by hand lay-up. Compos Sci Technol 64:289–297

15. Khashaba UA, Seif MA, Elhamid MA (2007) Drilling analysis of chopped composites. Compos Part A 38:61–70

16. Haykin S (2007) Neural networks: a comprehensive foundation, 2nd edn. Prentice-Hall of India Private Ltd, New Delhi

17. Rajasekaran S, VijayalakshmiPai GA (2007) Neural networks, fuzzy logic, and genetic algorithms: synthesis and applications. Prentice-Hall of IndiaPrivate Ltd, New Delhi

18. Himmel C, May G (1993) Advantages of plasma etch modeling using neural networks over statistical techniques. IEEE Trans Semicond Manuf 6:103–111

19. Bezerra EM, Ancelotti AC, Pardini LC, Rocco JAFF, Iha K, Ribeiro CHC (2007) Artificial neural networks applied to epoxy composites reinforced with carbon and E-glass fibers: analysis of the shear mechanical properties. Mater Sci Eng A 464:177–185

20. Hayajneh MT, Hassan AM, Mayyas AT (2009) Artificial neural network modelling of the drilling process of self-lubricated aluminium/alumina/graphite hybrid composites synthesized by powder metallurgy technique. J Alloys Compd. doi:10.1016/j.jallcom.2008.11.155

21. Kadi H (2006) Modeling the mechanical behavior of fiber-reinforced polymeric composite materials using artificial neural networks—a review. Compos Struct 73:1–23

22. Karnik SR, Gaitonde VN, Rubio JC, Correia AE, Abrao AM, Davim JP (2008) Delamination analysis in high speed drilling of carbon fibre reinforced plastic (CFRP) using artificial neural network model. Mater Des. doi:10.1016/j.matdes.2008.03.014

23. Tsao CC, Hocheng H (2007) Evaluation of thrust force and surface roughness in drilling composite material using Taguchi analysis and neural network. J Mater Process Technol. doi:10.1016/j.jmatprotec.2006.04.126

24. Hansda S, Banerjee S (2012) Multiple performance characteristics optimisation in drilling of glass fibre reinforced polyester composite at different weightage of performance by grey relational analysis. Int J Mach Mach Mater 2 12(1–2):14–27

25. Hansda S, Banerjee S (2014) Optimizing multi characteristics in drilling of GFRP composite using utility concept with Taguchi's approach. Proc Mater Sci 6:1476–1488

26. Soren H et al (2013) Analyzing process capability of drilling on glass fiber reinforced polyester (GFRP) composites with Taguchi Loss Function. Adv Mater Res 622. doi:10.4028/www.scientific.net/AMR.622-623.1314

27. Rajamurugan TV, Shanmugam K, Palanikumar K (2013) Analysis of delamination in drilling glass fiber reinforced polyester composites. Mater Des 45:80–87

28. Mishra R et al (2010) Neural network approach for estimating the residual tensile strength after drilling in uni-directional glass fiber reinforced plastic laminates. Mater Des 31(6):2790–2795

29. Tsao CC (2008) Comparison between response surface methodology and radial basis function network for core-center drill in drilling composite materials. Int J Adv Manuf Technol 37:1061–1068

30. Abrao AM, Faria PE, Rubio JC, Reis P, Davim JP (2007) Drilling of fibre reinforced plastics: a review. J Mater Process Technol 186:1–7
31. Babu J et al (2015) Assessment of delamination in composite materials: a review. Proc Inst Mech Eng Part B J Eng Manuf 0954405415619343. doi:10.1177/0954405415619343
32. Canakci A, Varol T, Ozsahin S (2015) Artificial neural network to predict the effect of heat treatment, reinforcement size, and volume fraction on AlCuMg alloy matrix composite properties fabricated by stir casting method. Int J Adv Manuf Technol 78(1–4):305–317
33. Satapathy A, Tarkes DP, Nayak NB (2010) Wear response prediction of TiO_2-polyester composites using neural networks. Int J Plast Technol 14(1):24–29
34. Varol T, Canakci A, Ozsahin S (2015) Modeling of the prediction of densification behavior of powder metallurgy Al–Cu–Mg/B4C composites using artificial neural networks. Acta Metall Sin (English Letters) 28(2):182–195
35. Khanlou HM et al (2015) Prediction and characterization of surface roughness using sandblasting and acid etching process on new non-toxic titanium biomaterial: adaptive-network-based fuzzy inference system. Neural Comput Appl 26(7):1751–1761
36. Khanlou HM et al (2014) Prediction and optimization of electrospinning parameters for polymethyl methacrylate nanofiber fabrication using response surface methodology and artificial neural networks. Neural Comput Appl 25(3–4):767–777
37. Sadollah A et al (2013) Prediction and optimization of stability parameters for titanium dioxide nanofluid using response surface methodology and artificial neural networks. Sci Eng Compos Mater 20(4):319–330
38. Hemmatian H et al (2013) Optimization of laminate stacking sequence for minimizing weight and cost using elitist ant system optimization. Adv Eng Softw 57:8–18
39. Kosko B (1994) Neural networks and fuzzy systems. Prentice-Hall of India Private Ltd, New Delhi
40. Schalkoff RB (1997) Artificial neural networks. McGraw-Hill, New York
41. Vankanti VK, Ganta V (2014) Optimization of process parameters in drilling of GFRP composite using Taguchi method. J Mater Res Technol 3(1):35–41